



# Dihydroartemisinin exhibits antitumor activity toward hepatocellular carcinoma *in vitro* and *in vivo*

Chris Zhiyi Zhang<sup>a,b,c</sup>, Haitao Zhang<sup>d</sup>, Jingping Yun<sup>a,b,\*\*</sup>, George Gong Chen<sup>c,\*</sup>, Paul Bo San Lai<sup>c</sup>

<sup>a</sup> State Key Laboratory of Oncology in Southern China, Sun Yat-Sen University Cancer Center, Guangzhou, China

<sup>b</sup> Department of Pathology, Sun Yat-Sen University Cancer Center, Guangzhou, China

<sup>c</sup> Department of Surgery, Prince of Wales Hospital, The Chinese University of Hong Kong, Shatin, N.T., Hong Kong

<sup>d</sup> Department of Biochemistry and Molecular Biology, Guangdong Medical College, Guangdong Province, China

## ARTICLE INFO

### Article history:

Received 3 January 2012

Accepted 1 February 2012

Available online 9 February 2012

### Keywords:

Dihydroartemisinin

Apoptosis

Mcl-1

Bak

Hepatocellular carcinoma

## ABSTRACT

Dihydroartemisinin (DHA), a semi-synthetic derivative of artemisinin isolated from the traditional Chinese herb *Artemisia annua* L., has been shown to exhibit inhibitory effects on human cancer cells. However, its antitumor ability toward hepatocellular carcinoma (HCC) has not been studied. In this study, we demonstrated that DHA significantly inhibited HCC cell growth *in vitro* and *in vivo* via inducing G2/M cell cycle arrest and apoptosis. The induction of p21 and the inhibition of cyclin B and CDC25C contributed to DHA-induced G2/M arrest. DHA-induced apoptosis was associated with mitochondrial membrane depolarization, release of cytochrome c, activation of caspases, and DNA fragmentation. Activation of caspase 9 and caspase 3, but not caspase 8, was detected in DHA-treated cells. Attenuation of apoptosis in cells pretreated with Z-VAD-FMK suggested the involvement of caspase cascade. Furthermore, p53 facilitated apoptosis caused by DHA. Bcl-2 family proteins were also responsible for DHA-induced apoptosis. DHA exposure decreased Mcl-1 expression but increased the levels of Noxa and active Bak. Bak was released from the Mcl-1/Bak complex due to the decline of Mcl-1. Further study revealed that Mcl-1 was rapidly degraded in DHA-treated cells and that DHA-induced apoptosis was largely inhibited by overexpression of Mcl-1 or RNAi-mediated decrease of Bak and Noxa. In a HCC-xenograft mouse model, the intraperitoneal injection of DHA resulted in significant inhibition of HCC xenograft tumors. Taken together, our data, for the first time, demonstrate the potential antitumor activity of DHA in HCC.

© 2012 Elsevier Inc. All rights reserved.

## 1. Introduction

Hepatocellular carcinoma (HCC) is a malignancy of worldwide significance and is currently one of the most common solid tumors and the third leading cause of cancer-related death [1]. The incidence of HCC geographically varies, due to the large heterogeneity of the penetration of the risk factors within the population. About 80% of new cases occur in developing countries, but the incidence is increasing in economically developed regions, including Japan, Western Europe, and the United States [2,3]. HCC is frequently associated with liver cirrhosis and liver dysfunction, making the treatment of HCC more difficult than many other cancers [4,5]. To date, surgery is still the most effective treatment with curative potential, but only about 20% of patients with HCC

are eligible for surgical intervention [6,7]. Therefore, numerous approaches have been conducted to search for other options such as efficient chemotherapeutic agents. Since apoptotic resistance is a major challenge that hampers the efficacy of anticancer treatment, accumulating attention has been paid to the development of innovative compounds that increase the death of therapy-resistant tumor cells, such as HCC cells [8].

One of the promising approaches for anti-HCC agent development is drug screening from natural products, such as components from traditional Chinese medicine. Artemisinin, the active ingredient derived from Chinese medicinal herb *Artemisia annua* L., is a safe and effective FDA-approved and WHO-recommended mainstay in treating malaria [9,10]. Recent studies have suggested that artemisinin also exerts preferentially cytotoxic effects on human cancers. Dihydroartemisinin (DHA, CAS 71939-50-9), the main active metabolite of artemisinin derivatives, has been demonstrated to exhibit antitumor effects toward various human cancers, including lung, ovarian, and pancreatic cancer [11–13]. For example, Ji et al. [14] reported that DHA inhibited proliferation of osteosarcoma cells via inducing the expression of cyclin D1 and

\* Corresponding author. Tel.: +852 2632 3934; fax: +852 2645 0605.

\*\* Corresponding author. Tel.: +86 20 8734 3601x815.

E-mail addresses: [yunjp@mail.sysu.edu.cn](mailto:yunjp@mail.sysu.edu.cn) (J. Yun), [gchen@cuhk.edu.hk](mailto:gchen@cuhk.edu.hk) (G.G. Chen).

Bax and inhibiting the activity of NF- $\kappa$ B. Handrick et al. [15] showed that DHA induced apoptosis via the intrinsic pathway in lymphoma cells. Gao et al. [16] demonstrated that DHA exhibited the anti-leukemic activity through inactivating MEK/ERK pathways. However, the detailed mechanism through which DHA inhibits cancer growth is not fully understood. Furthermore, the effect of DHA on HCC has not been studied.

In the present study, we investigated the antitumor effect of DHA, a semi-synthetic derivative of artemisinin, on HCC *in vitro* and *in vivo*. We found that DHA displayed cytotoxicities against HCC cells via inducing G2/M arrest and apoptosis. Induction of p21 and subsequent inhibition of cyclin B and CDC25C contributed to DHA-induced G2/M phase arrest. DHA-induced apoptosis was associated with the activation of caspases and PARP, mitochondrial membrane depolarization and cytochrome c release. Furthermore, p53 significantly facilitated DHA-induced apoptosis which required Mcl-1 degradation and Bak activation. Moreover, the *in vivo* efficacy of DHA on Hep G2-bearing nude mice revealed a significant remission of the xenograft tumor. Taken together, our data, for the first time, have revealed the potential antitumor effect of DHA on HCC.

## 2. Materials and methods

### 2.1. Cell culture and transfection

Human HCC cell lines (Hep G2, PLC/PRF/5 and Hep3B) were purchased from American Type Culture Collection (ATCC, Manassas, VA) and cultured in Dulbecco's modified Eagle's medium (DMEM) (Gibco, Gaithersburg, MD) containing 10% fetal bovine serum (FBS), 100 mg/ml penicillin, and 100 mg/ml streptomycin in a humidified atmosphere of 5% CO<sub>2</sub> and 95% air at 37 °C. Cells were seeded in 6-well plate for 24 h, and then transfected with pCDNA 3.1, pCDNA 3.1-Mcl-1, pCDNA 3.1-p53, according to the manufacture's instruction of Lipofectamine 2000 (Invitrogen, Carlsbad, CA).

### 2.2. Antibodies and reagents

Primary antibodies for cyclin A, cyclin B, cyclin E, Beclin 1, Mcl-1, Bcl-xL, Bid, p53, PARP, Bak,  $\beta$ -Actin, Actin, COX-VI and GAPDH were purchased from Santa Cruz Biotechnology (Santa Cruz, CA). Antibodies for CDC25C, ATG-5, LC3, active Bak, caspase 8, caspase 9, caspase 3, p21, Bcl-2, cytochrome c, Bax, and Noxa were provided by Cell Signaling (Danvers, MA). Dihydroartemisinin (dissolved in DMSO), Cycloheximide (CHX, dissolved in DMSO) and the caspase inhibitor (Z-VAD-FMK, dissolved in DMSO) were purchased from Sigma (St. Louis, MO).

### 2.3. MTT

Cell viability was assessed by 3-(4, 5-dimethylthiazol-2-yl)-2, 5-diphenyltetrazolium bromide (MTT) assay. Briefly,  $8 \times 10^3$  of cells were seeded into 96-well plates for 24 h, followed by incubation with various doses of DHA for indicated time. After adding 100  $\mu$ l/well of MTT solution, the cells were incubated for another 2 h. Supernatants were then removed and the formazan crystals were dissolved in 100  $\mu$ l/well DMSO. The absorbance at 570/630 nm of each sample was measured using multilabel plate reader (PerkinElmer). Three independent experiments were performed.

### 2.4. Colony formation

One hundred of cells were seeded into 6-well plates, and cultured for 5 d. And then the medium was replaced by fresh one containing DHA. After being incubated for another 5 or 10 d, colony formed by HCC cells was stained with 0.05% crystal violet (Sigma, St. Louis, MO) for 8 min. The number of colony was then quantified.

### 2.5. Cell cycle analysis

Following DHA treatment for indicated periods, HCC cells were washed with ice-cold PBS, and fixed with 70% ethanol at 4 °C for overnight. Ethanol was removed. Cells were re-suspended in PBS containing PI (50  $\mu$ g/ml, Sigma) and RNase A (50  $\mu$ g/ml, Sigma) for 30 min in dark. And then cells were subjected to flow cytometry (FACS Vantage, Becton Dickinson, Franklin Lakes, NJ). The percentage of cells at each cell cycle phase was analyzed.

### 2.6. Western blot

Cell lysates were boiled with 6 $\times$  sodium dodecyl sulfate (SDS) loading buffer and then fractionated by SDS-PAGE. The proteins were transferred to PVDF membrane which was then incubated with a primary specific antibody in 5% of non-fat milk, followed by a horse radish peroxidase (HRP)-conjugated anti-mouse or anti-rabbit second antibodies. ECL detection reagent (Amersham Life Science, Piscataway, NJ) was used to demonstrate the results.

### 2.7. Morphological analysis

To evaluate the apoptotic activity of DHA, we performed nuclear staining, using the DNA-binding dye Hoechst-33342. Cells were plated and exposed to DMSO, or 40  $\mu$ M DHA for 24 h. Cells were then fixed with 4% PFA in PBS for 10 min. Fixed cells were washed with PBS, incubated with Hoechst-33342 (10  $\mu$ g/ml, Sigma, St. Louis, MO) for 15 min in dark. Apoptotic cells were identified by condensation of chromatin and fragmentation of nuclei under a fluorescent microscope. Images were taken, using a camera Qimaging (Burnaby, BC, Canada).

### 2.8. TUNEL assay

Apoptosis assay was performed using Apo-Direct TUNEL Assay kit (Millipore, Billerica, MA). Cells were harvested and fixed in 4% PFA for 60 min at 4 °C, followed by a second fixation in 70% (v/v) ethanol overnight at –20 °C. Cells were then treated with various reagents for a designed period according to the manufacture's instruction. Finally, cells were analyzed by flow cytometry using FACS Vantage machine (Becton Dickinson). The Cell Quest software (Verity Software House) was used to analyze the data.

### 2.9. In situ cell death detection

Labeling of fragmented DNA to assess apoptosis was performed with TUNEL staining (green fluorescence), using *In Situ* Cell Death Detection Kit (Roche, Indianapolis, IN), as described in our previous study [17].

### 2.10. Mitochondrial membrane depolarization

Changes of mitochondrial transmembrane potential (lower  $\Delta\Psi_m$ ) in HCC cells induced by DHA were measured using the same procedure as our previous study with JC-1 (Sigma, St. Louis, MO) staining at a dose of 2.5  $\mu$ g/ml.

### 2.11. RNA interference

Small interfering RNAs (Invitrogen, Carlsbad, CA) for p53 (si-p53), Mcl-1 (si-Mcl-1), Bak (si-Bak), and Noxa (si-Noxa) were synthesized as 5'-GACUCCAGUGGUAU CUAC-3', 5'-GCATCGAACCATTAGCAGA-3', 5'-GUACGAAGAUUCUCAA U-3', and 5'-GGAGAUUUGGAGACAAA CU-3', respectively. Nonspecific siRNA (si-ctrl) was also designed. For RNA interference,  $2 \times 10^5$  of cells were seeded into 6-well Plates 24 h prior to transfection. For each well, 30 nM siRNA was

transfected into cells by Lipofectamine 2000 according to the manufacturer's protocol. After 24 h, the cells were ready for gene knockdown analysis.

## 2.12. Measurement of caspase 3 activity

The activity of caspase 3 induced by DHA treatment was determined by the Caspase-3 Activity Assay Kit (Merck, Darmstadt, Germany).

## 2.13. Immunofluorescence

Cells grown on cover slips were fixed for 20 min in PBS containing 4% PFA, permeabilized in 0.1% Triton X-100 for 5 min twice and incubated in blocking buffer (3% donkey serum in TBS) for 1 h. Cells were then incubated in dilution buffer (3% bovine serum albumin in TBS) containing the indicated primary antibody for active Bak for 2 h in room temperature and then washed extensively in PBS before being incubated with the appropriate fluorochrome-conjugated secondary antibody for 1 h. DNA was stained by 4',6-diamidino-2-phenylindole (DAPI, Sigma).

## 2.14. Immunoprecipitation

Cells were lysed in 1% CHAPS (Cell Signaling, Danvers, MA) buffer supplemented with proteinase inhibitor cocktail. The specific antibody for Mcl-1 was added and incubated for 2–3 h at 4 °C, and then protein A/G beads were added for an additional 2 h. Precipitated proteins were dissolved in the SDS loading buffer and fractionated by SDS-PAGE.

## 2.15. Immunohistochemistry

Formalin-fixed and paraffin-embedded HCC sections with a thickness of 4  $\mu$ m were dewaxed in xylene and graded alcohols, hydrated, and washed in phosphatebuffered saline (PBS). After pretreatment in a microwave oven, endogenous peroxidase was inhibited by 3% hydrogen peroxide in methanol for 20 min, followed by avidin-biotin blocking using a biotin-blocking kit (DAKO, Hamburg, Germany). Slides were then incubated with antibodies for p53, Mcl-1, active Bak, and cleaved caspase 3 for 4 h in a moist chamber at room temperature, washed in PBS, and incubated with biotinylated goat anti-rabbit/mouse antibodies. Slides were developed with the Dako Liquid 3,3'-diaminobenzidine tetrahydrochloride (DAB) + Substrate Chromogen System and counterstained with hematoxylin.

## 2.16. Animal studies

$1 \times 10^7$  of Hep G2 cells were suspended in sterile PBS and injected subcutaneously into the right flank of the mice. Mice were checked daily for xenograft/tumor development. Mice were randomized into three groups of 6 mice/group. The DHA group received intraperitoneal injection of 20 mg DHA/kg of mouse body weight, five times a week. The control group was given normal saline, and the DMSO group received an equal volume of solvent control. After treatment at various time intervals, mouse body weight and tumor size were measured. Finally, tumors were excised, weighed and fixed in 4% of PFA. Paraffin-embedded tissues were then sectioned at 4  $\mu$ m and ready for immunohistochemistry and TUNEL assay.

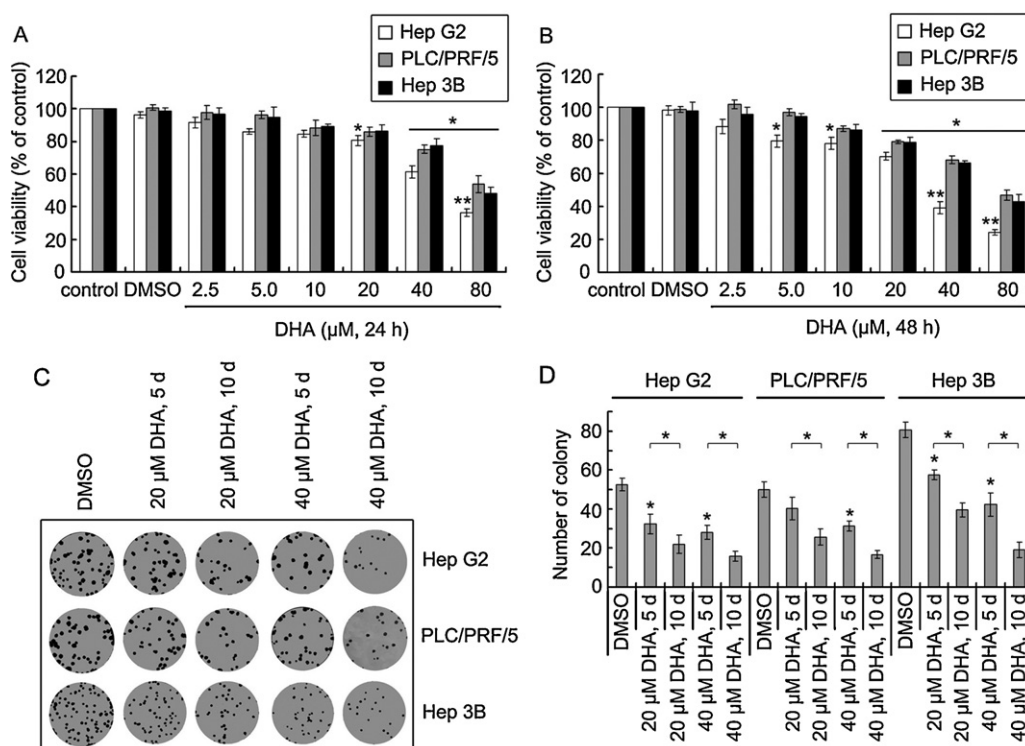


**Fig. 1.** DHA exerted cytotoxic activity in HCC cells. (A) DHA induced HCC cell death in a dose-, and time-dependent manner. HCC cells (Hep G2, PLC/PRF/5 and Hep3B) were treated with various concentrations of DHA (0–80  $\mu$ M) for 24 h. Cell viability was determined by MTT assay. (B) Cytotoxicities of DHA at various doses in HCC cells for 48 h were measured. Data represent mean  $\pm$  SD of three independent experiments. \* $P$  < 0.05 and \*\* $P$  < 0.01, versus the control group. (C) The inhibitory effect of DHA on HCC cell growth was further confirmed by colony formation assay. One hundred of cells were seeded into 6-well plates for 7 d, and then cultured with either DMSO or DHA at indicated doses for another 5 d and 10 d. Colonies were stained with 0.05% crystal violet. A representative result was shown. (D) Number of colony in each well was counted and statistical analysis was performed. Data are mean  $\pm$  SD of three independent experiments. \* $P$  < 0.05, versus the DMSO group.

### 2.17. Statistical analysis

Difference between groups was determined for statistical significance using one-way ANOVA or Student's *t*-test. All *P*-values are two-sided and *P* < 0.05 was considered as statistically significant. All statistical calculations were performed with the SPSS software (SPSS, Inc., Chicago, IL). The data were presented as mean ± SD from at least three independent experiments.

## 3. Results

### 3.1. Cytotoxicity of DHA toward HCC cells

To study the *in vitro* antitumor effect of DHA on HCC cells, cells were exposed to various concentrations (0–80 μM) for 24 and 48 h. As indicated in MTT results, DHA induced cytotoxicity in a dose- and time-dependent manner (Fig. 1A and B). It was noted that at 24 h of exposure to DHA, 20 μM DHA caused remarkable cell death in Hep G2 but not in PLC/PRF/5 and Hep 3B cells, whereas 40 μM DHA induced significant cell death (Fig. 1A) in all 3 cell lines. Therefore, DHA at concentrations of 20 μM and 40 μM were used in the subsequent experiments.

The anti-HCC property of DHA in HCC cells was also determined by colony formation assay. Cells in control groups formed a number of visible colonies in 15 d. Compared to the DMSO group, the number of colony formed by cells cultured with DHA was significantly lower and the size was much smaller (Fig. 1C). Furthermore, the prolonged treatment of DHA markedly reduced both the number and the size of colony (Fig. 1D). These data, plus the MTT results, revealed that DHA had potential anti-HCC properties by reducing the proliferation as well as the viability of tumor cells.

### 3.2. DHA induces G2/M arrest in HCC cells

We then examined whether DHA could affect the cell cycle of HCC cells. Following DHA treatment, all three types of HCC cells were noticeably arrested in G2/M phase (Fig. 2A). However, patterns of cell cycle phase distribution differed among the three cell lines tested. For instance, there was a significant reduction of G1 phase cells in Hep G2 but not in PLC/PRF/5 cells where a dramatic decrease of cells in S phase was recorded (Fig. 2B). Western blot was next performed to investigate the possible mechanism through which DHA induced cell cycle arrest (Fig. 2C).

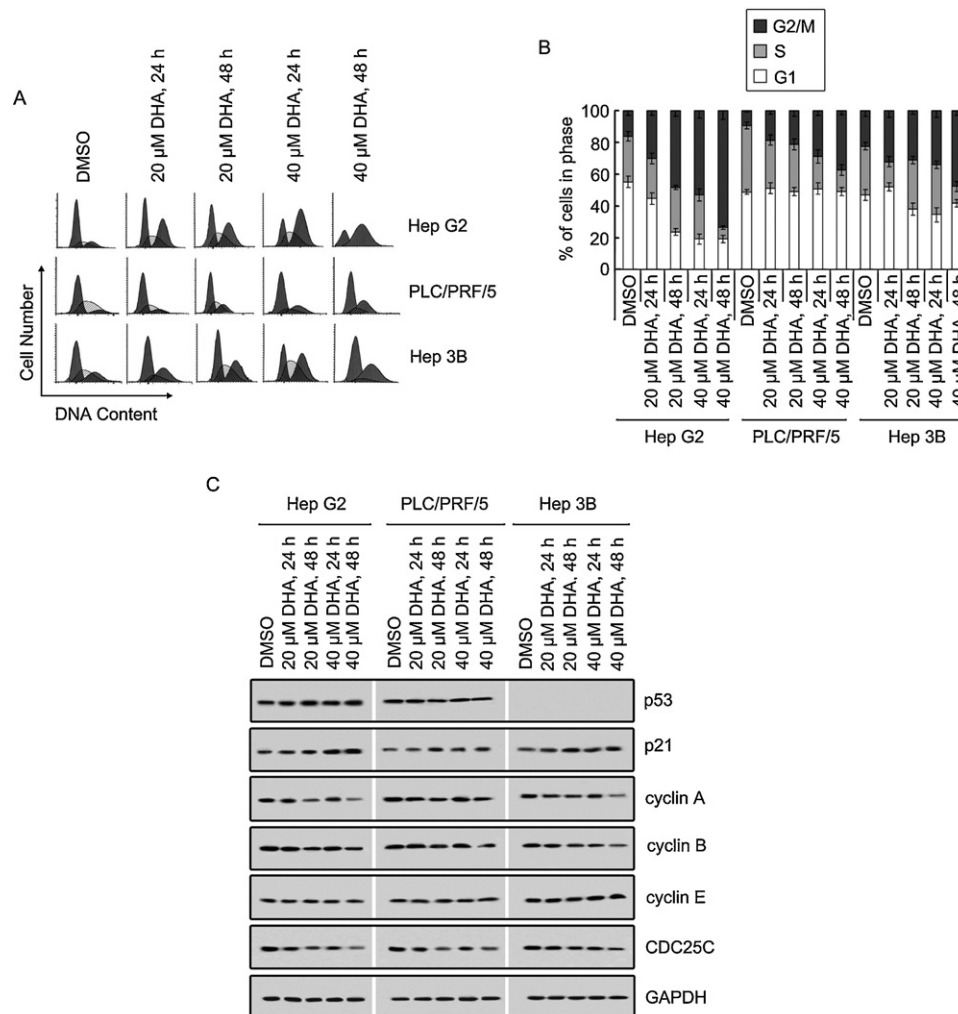


**Fig. 2.** DHA induced G2/M arrest in HCC cells. (A) G2/M arrest was induced by DHA treatment in HCC cells. Cells were treated with DHA for 24 and 48 h. After being stained with propidium iodide, cells were subjected to flow cytometry to measure DNA contents. A representative image of flow cytometry was shown. (B) Quantitative analysis of cells in each cell cycle phase was performed. The experiment was repeated three times in triplicate. Data represent mean ± SD. (C) p21 induction contributed to DHA-induced G2/M arrest. HCC cells were incubated with DHA for 24 and 48 h. Proteins were extracted and subjected to Western blot analysis to examine molecules involved in cell cycle regulation, including p53, p21, cyclin A/B/E, and CDC25C. GAPDH was served as a loading control.

In response to DHA treatment, wild-type p53 (present in Hep G2 cells) increased slightly, while mutant p53 (present in PLC/PRF/5 cells) was decreased. Induction of p21 was found and the subsequent inhibition of cyclin A and cyclin B was also detected. The level of CDC25C, which is essential for entrance into mitosis, reduced in DHA-treated cells. However, the protein levels of cyclin E and cyclin D1 were hardly affected (Fig. 2C and data not shown).

### 3.3. DHA induces apoptosis in HCC cells

Next we characterized the pro-apoptotic activity of DHA. DHA treatment potently induced apoptosis in HCC cells, which was shown by TUNEL assays indicating a time- and concentration-dependent

increase in TUNEL-positive cells (Fig. 3A). Compared with control, treatment with 20  $\mu$ M DHA increased apoptotic cells by 3.2–8.7-fold in three HCC cells (Fig. 3B). Interestingly, the potency of DHA at 20  $\mu$ M to induce apoptosis in HCC cells was different, with Hep G2 being most sensitive and Hep3B cells being least sensitive (Fig. 3B). The DHA-induced apoptosis was further confirmed by Hoechst 33342 staining in HCC cells exposed to 40  $\mu$ M DHA for 24 h, showing characteristic features including chromatin condensation and apoptotic body (Fig. 3C and D).

To elucidate the possible mechanism via which DHA induced apoptosis, the activation of caspase cascade was examined. Western blot analysis revealed that caspase 9, but not caspase 8, was activated in cells exposed to DHA (Fig. 3E). The subsequent activation of

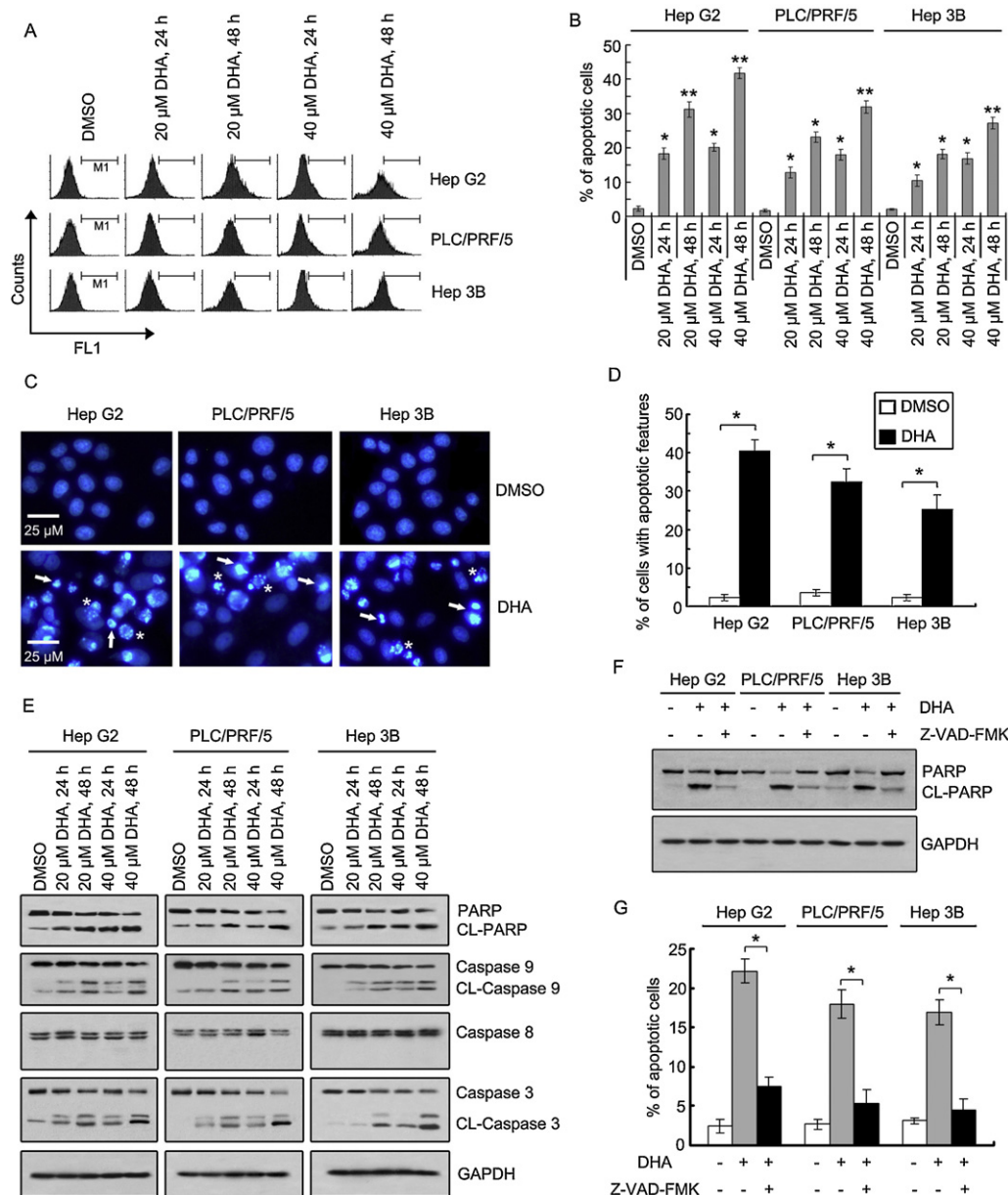


**Fig. 3.** DHA induced apoptosis in HCC cells. (A) Apoptotic cells were increased in DHA-treated HCC cells. Cells were cultured with DHA for indicated time and then subjected to TUNEL assay, using flow cytometry. Representative images were presented. (B) The percentage of apoptotic cells were shown. Data were mean  $\pm$  SD of three independent experiments. \* $P$  < 0.05 and \*\* $P$  < 0.01, versus the DMSO group. (C) DHA treatments resulted in the production of apoptotic body. Cells treated with 40  $\mu$ M DHA for 24 h were stained with Hoechst 33342 dye, and apoptotic bodies (indicated by asterisks) and chromatin condensation (denoted by arrows) were revealed under a fluorescence microscope. (D) Contemporarily, the number of cells with apoptotic features was determined and the percentage was indicated by histogram. \* $P$  < 0.05. (E) Activations of caspase 3, caspase 9 and PARP, but not caspase 8, were involved in DHA-induced apoptosis. HCC cells were treated with DHA at 20 and 40  $\mu$ M for 24 and 48 h. Western blot was performed to examine the levels of caspases and PARP, as well as their active forms. (F) DHA induced apoptosis in a caspase-dependent fashion. Cells were pretreated with caspase inhibitor, Z-VAD-FMK, for 2 h, and then incubated with 40  $\mu$ M DHA for another 24 h. Activation of PARP was determined by Western blot to assess the apoptosis. (G) Cells treated as described in (F) were subjected to TUNEL assay to further confirm the DHA-induced apoptosis. Data were mean  $\pm$  SD of three independent experiments. \* $P$  < 0.05.



caspase 3 and the resulting cleavage of PARP were also detected. These data suggest that DHA induced apoptosis through the intrinsic but not the extrinsic pathway. Pretreatment with 20  $\mu$ M Z-VAD-FMK markedly attenuated the activation of PARP (Fig. 3F). TUNEL assay further indicated a significant decline of DHA-induced apoptosis, demonstrating an essential role of caspase cascade (Fig. 3G).

#### 3.4. Exposure to DHA resulted in mitochondrial membrane depolarization (MMD) and release of cytochrome *c*

Since DHA induced apoptosis through the intrinsic pathway and it is mitochondrial-dependent [18], we next intended to examine

whether DHA treatment would lead to the depolarization of mitochondrial outer membrane. Cells exposed to DHA were stained with JC-1 and subjected to flow cytometry. Results showed that DHA treatment remarkably lowered the mitochondrial transmembrane potential, resulting from mitochondrial membrane depolarization (Fig. 4A).

MMD is usually associated with the release of cytochrome *c* from mitochondria to cytoplasm. We next measured the expression of cytochrome *c* in cytosolic and mitochondrial fractions. Results demonstrated a gradual increase and a steady decrease of cytochrome *c* expression in cytoplasm and mitochondrial, respectively, in DHA-exposed HCC cells (Fig. 4B).

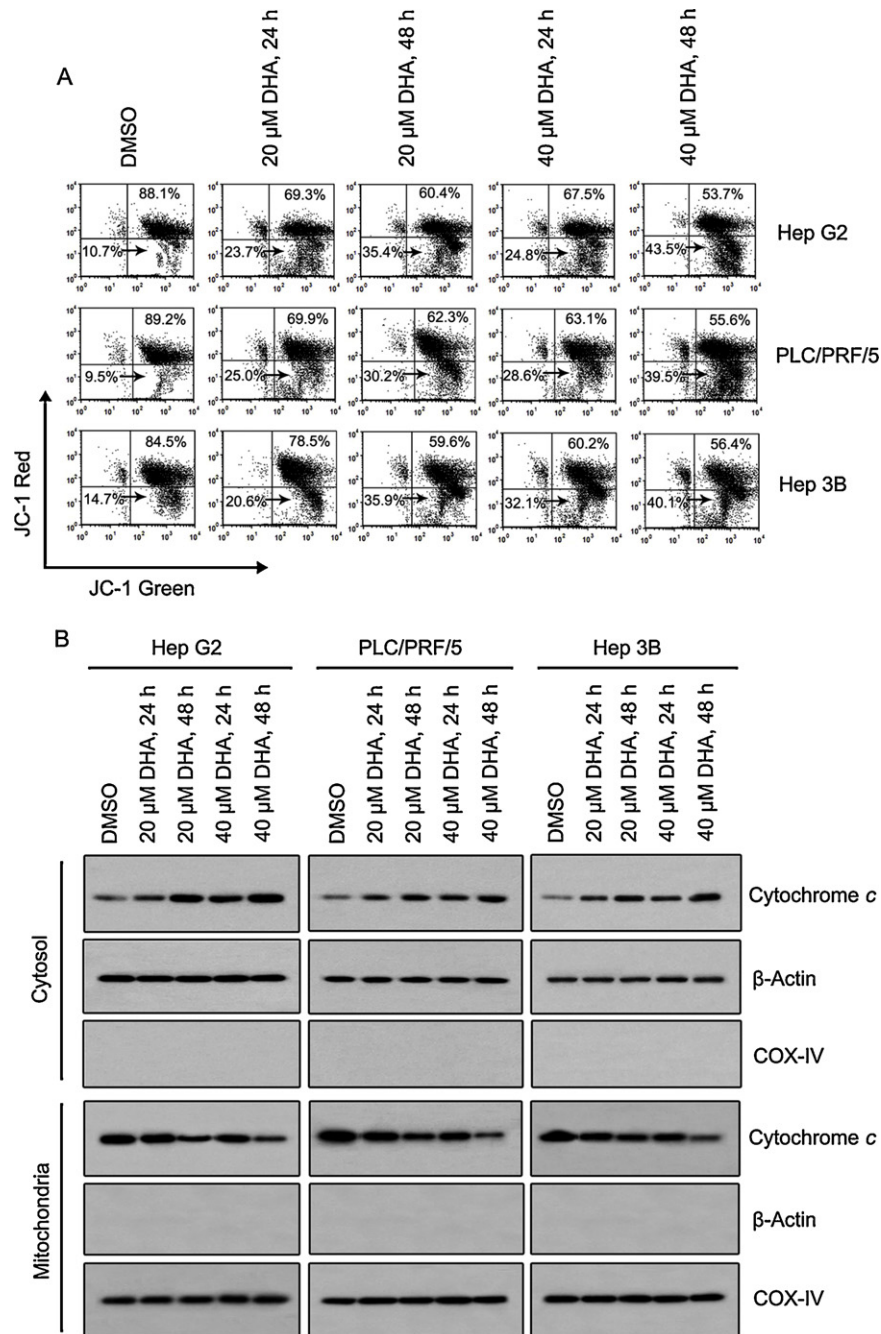


**Fig. 4.** DHA induced mitochondrial membrane depolarization and release of cytochrome *c*. (A) DHA induced MMD in HCC cells. Cells were treated with DHA for indicated periods, stained with JC-1 and analyzed by flow cytometry to determine the breakdown of  $\Delta\psi_m$  to indicate MMD. A representative result was shown. (B) Cytochrome *c* was released to cytosol in DHA-treated cells. HCC cells were treated with DHA for 24 and 48 h. Fractions of cytosol and mitochondria were isolated to examine the distribution of cytochrome *c*.  $\beta$ -Actin and COX-IV were used as the markers for the cytosol and the mitochondria, respectively.

### 3.5. p53 facilitates DHA-induced apoptosis in HCC cells

Our previous data including MTT and TUNEL results indicated that Hep G2 cells were more sensitive to DHA treatment than the other two cell lines. In view of an obvious difference among these HCC cells lies in the p53 status, with wild type p53 in Hep G2, mutant p53 in PLC/PRF/5, and no p53 in Hep3B, we examined the role of p53 in DHA-induced apoptosis. In Hep G2 cells, p53 was eliminated by p53 siRNA (Fig. 5A), while p53 was introduced into Hep3B cells (Fig. 5B). The result of MTT assay showed that the downregulation of p53 partly inhibited the DHA-induced cell death in Hep G2 cells, whereas the ectopic expression of p53 in Hep3B cells significantly reduced cell viability (Fig. 5A and B). Furthermore, less apoptotic cells were present in p53-deficient Hep3B cells, but more were shown in p53-overexpressing Hep3B cells, following 40  $\mu$ M DHA for 24 h (Fig. 5C). This was further confirmed by TUNEL assay showing a clear difference in the percentages of apoptotic cells (Fig. 5D). In line with the increased

apoptosis, caspase 3 activity was higher in cells with wild type p53 (Fig. 5E).

### 3.6. Mcl-1 degradation and Bak activation were associated with DHA-induced apoptosis

Bcl-2 family proteins are involved in caspase-dependent apoptosis [19]. We thus examined the role of Bcl-2 family proteins in DHA-induced apoptosis by Western blot (Fig. 6A). Results showed that DHA exposure noticeably reduced the levels of Mcl-1 and Bcl-2, but induced Noxa expression. However, DHA treatment did not affect the levels of Bax, Bid and Bcl-xL. Although Bak, detected by Western blot using an antibody recognizing total Bak, showed different reactions in response to DHA treatment in three HCC cell lines: increased in Hep G2 and PLC/PRF/5 but unchanged in Hep3B cells (Fig. 6A), data of immunofluorescence, using antibody only recognizing active Bak, revealed that Bak was activated in all three cell lines (Fig. 6B).

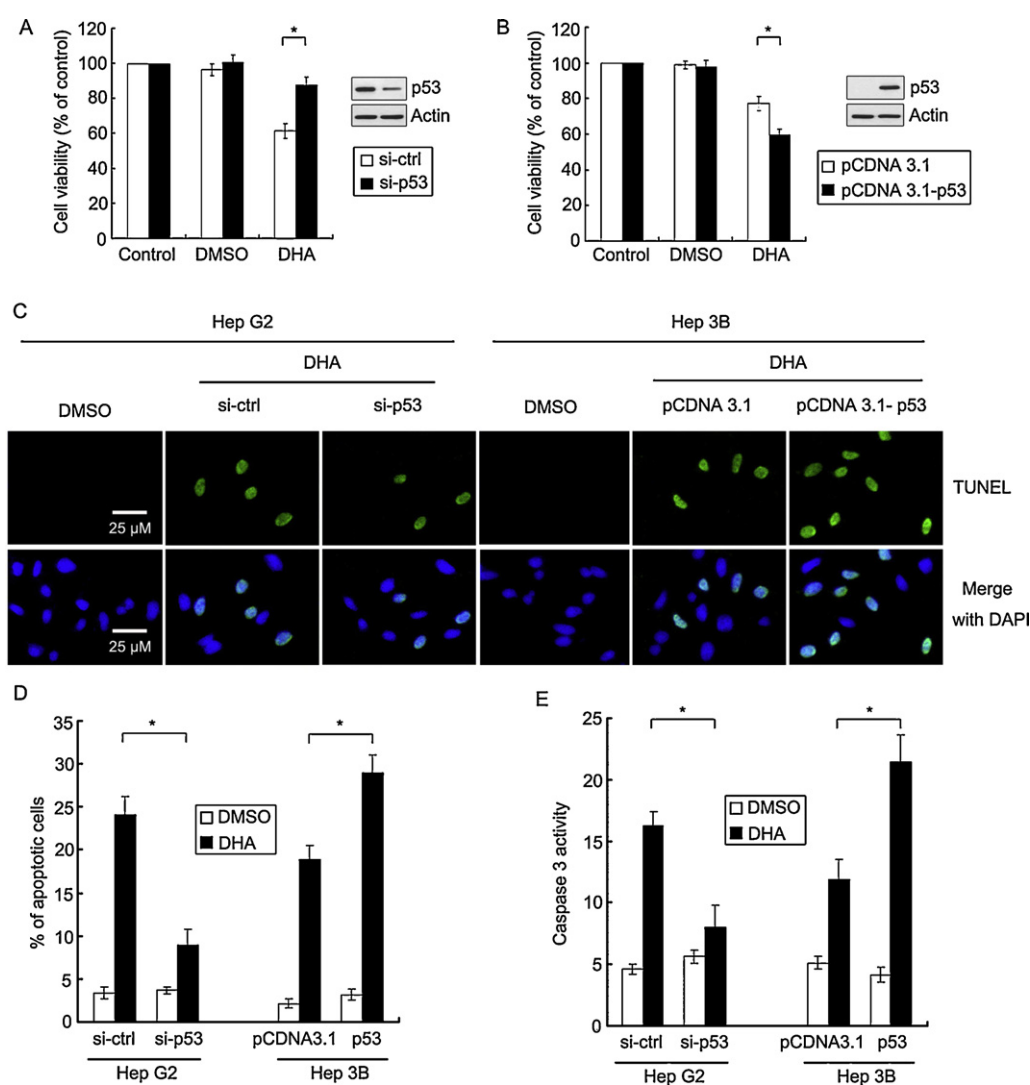


**Fig. 5.** p53 facilitated DHA-induced apoptosis. (A) Decrease of p53 trailed off the cytotoxicity of DHA in Hep G2 cells. Cells were transfected with control or p53 siRNA for 18 h, and then treated with 40  $\mu$ M DHA for another 24 h. Cell viability was determined by MTT assay. (B) Expression of p53 in Hep3B cells potentiated DHA-induced apoptosis. Cells were transfected with pCDNA 3.1 or pCDNA 3.1-p53 for 18 h, and then treated with 40  $\mu$ M DHA for another 24 h. Cell viability was determined by MTT assay. (C) The effect of p53 on DHA-induced apoptosis was measured by TUNEL assay, using *in situ* cell death detection kit. Cells treated as described in (A) and (B) were subjected to TUNEL assay. Apoptotic cells were revealed under fluorescent microscope. (D) The effect of p53 on DHA-induced apoptosis was further confirmed by TUNEL assay, using flow cytometry. Percentage of apoptotic cells was recorded. (E) Caspase 3 activation was involved in p53-mediated apoptosis in cells treated with DHA. The activity of caspase 3 in cells treated as described in (A) and (B) was determined and the relevant change was shown. For (A), (B), (D) and (E), data are mean  $\pm$  SD of three independent experiments. \* $P < 0.05$ .

In order to determine the role of Mcl-1, Bak and Noxa in DHA-induced apoptosis, we knocked down their levels with corresponding siRNA. Results demonstrated that activation of PARP was enhanced in cells with Mcl-1 elimination, but greatly attenuated in cells with Bak or Noxa elimination (Fig. 6C). The potency of p53 in DHA-mediated PARP cleavage was also elucidated (Fig. 6C). Next, TUNEL assay was performed using *in situ* cell death detection kit and flow cytometry to further evaluate the importance of these proteins in DHA-induced apoptosis (Fig. 6D). Data indicated that once Mcl-1 was downregulated, more dead cells were observed in DHA-treated HCC cells. In contrast, when Bak or Noxa was knocked down, cells were more resistant to DHA treatment (Fig. 6E). Finally, MTT assay demonstrated that the cytotoxicity of DHA was enhanced in cells treated with Mcl-1 siRNA but weakened in cells treated with Bak or Noxa siRNA. These data may indicate the requirement of Bak or Noxa for the maximal apoptosis induced by DHA, and the protective role of Mcl-1 in DHA-induced apoptosis (Fig. 6F).

### 3.7. Bak is released from Mcl-1/Bak suppressor complex following DHA treatment

It is well-documented that Mcl-1 is a potential suppressor of Bak via direct binding to Bak to inhibit its activation [20–22]. To investigate whether the degradation of Mcl-1 was associated with Bak activation, we performed immunoprecipitation to detect the interaction between Mcl-1 and Bak (Fig. 7A). Following exposure to 40  $\mu$ M DHA for 12 h, cells were lysed in 1% CHAPS buffer and proteins were subjected to immunoprecipitation and Western blot. Results showed that the level of Bak was slightly increased while the expression of Mcl-1 was rapidly decreased in the whole cell lysates. Next we examined the binding of Mcl-1 to Bak. Results revealed that after exposure to DHA, the Mcl-1-bound Bak was remarkably decreased to 53%, 57% and 61% of the original levels in Hep G2, PLC/PRF/5 and Hep3B cells respectively, which indicated that Bak was released from the Mcl-1/Bak suppressed complex due to the decrease of Mcl-1. This may be further proved by the data that the amount of Bak in cell lysates after immunoprecipitation was noticeably increased by 1.34–2.31-fold (Fig. 7B). Our finding is in line with a recent report that the degradation of Mcl-1 contributes to the efficacy of antitumor agents, such as cycloheximide and *Pseudomonas* exotoxin A [23].

To further confirm the role of Mcl-1 in DHA-mediated Bak activation and apoptosis, we examined the effect of DHA on the half-life of Mcl-1, using cycloheximide (CHX, a protein synthesis inhibitor). Results showed that the half-life of Mcl-1 was remarkably shorter with DHA stimulation in HCC cells (Fig. 7C and data not shown), which may suggest a rapid degradation of Mcl-1 in DHA-treated cells. Next we tested whether the overexpression of Mcl-1 could prevent DHA-induced apoptosis. As expected, Mcl-1 overexpression significantly abrogated the apoptosis caused by DHA treatment in all three HCC cell lines (Fig. 7D). This result was consistent with our previous data that Mcl-1 siRNA greatly enhanced the DHA-induced apoptosis. Accordingly, we concluded that Mcl-1 is an important initiator in DHA-mediated cell death.

### 3.8. DHA exhibited antitumor effect on Hep G2 xenograft

Having demonstrated the ability of DHA to kill HCC cells *in vitro*, we further determined its antitumor activity *in vivo*. Tumor xenograft was established through subcutaneous inoculation in nude mice with Hep G2 cells. Mice were treated with DHA. On Day 10, 18 and 26, DHA halted tumor growth respectively by 22%, 44% and 60%, compared to the control groups (Fig. 8A). On Day 28, mice were sacrificed and the tumor weights were measured. Unsurprisingly, DHA significantly reduced the weights of Hep G2 xenografts,

compared with control (Fig. 8B). These data suggest that DHA exhibited antitumor activity toward HCC *in vivo*. In order to test whether DHA treatment would result in apoptosis, tumor tissues were sectioned and subjected to *in situ* cell death detection. Results showed that the proportion of apoptotic cells was markedly increased from  $5.6 \pm 1.3\%$  in control group to  $18.6 \pm 5.2\%$  in DHA group (Fig. 8C and D). In addition, we performed immunohistochemistry to detect the proteins involved in DHA-induced apoptosis (Fig. 8E). Detectable difference of p53 expression was not observed. A striking increase of active Bak and a predominant decline of Mcl-1 were present in DHA-treated xenograft. Cleaved caspase 3 was also noticeably upregulated. Taken together, these data indicated that DHA manifested its antitumor effects, at least partly, through induction of Bak.

## 4. Discussion

Recent studies have suggested artemisinin and its semisynthetic derivatives (e.g., DHA) are potential candidates to treat cancer, due to their growth inhibitory activities toward human malignancies, such as lung cancer and metastatic melanoma [11,24,25]. However, the antitumor effect of DHA has not been investigated in HCC, and the molecular details of DHA-induced cell growth inhibition are not clearly understood. Here, we demonstrated that DHA exhibited antitumor activity toward HCC *in vitro* and *in vivo*. DHA exerted cytotoxicity in HCC cell lines, leading to G2/M cell cycle arrest and apoptosis. On the other hand, DHA significantly halted HCC xenograft tumor growth. These data suggest DHA may be a promising chemotherapeutic agent in HCC treatment.

In this study, DHA treatment increased p21, arrested cells at G2/M phase and decreased the levels of cyclin B and CDC25C. Cyclin B, essential for G2 to M transition, can interact with CDC2 to form cyclin B/CDC2 complex that is termed M phase-promoting factor (MPF) [26]. Cyclin B/CDC2 complexes are normally maintained inactive by phosphorylation of CDC2. However, MPF could be activated by some exogenous factors, such as CDC25C that is capable of dephosphorylating CDC2 [27–29]. Therefore, it is possible that the downregulation of CDC25C and the subsequent loss in cyclin B/cdc2 kinase activity contribute to DHA-induced G2/M arrest. Our data also indicated that DHA-induced G2/M phase arrest was p53-independent. In line with this finding, Kim et al. [30] demonstrated that TPA induced G2/M arrest by increasing p21 expression in a p53-independent manner. Jo et al. [31] showed that reversible G2/M arrest in colon cancer caused by diallyl disulfide (DADS) was p53-independent. In other studies, G2/M phase arrest has been demonstrated to be p53-dependent. Manna et al. [32] revealed that benfur exhibited antitumor activities via inducing G2/M arrest through p53-dependent mechanism. Meng et al. [33] reported that GNL3L depletion triggers G2/M arrest in p53-wild-type HCT116 cells but not in p53-null cells. Collectively, our data indicated that the upregulation of p21 but the downregulation of cyclin B and CDC25C contributed to DHA-induced G2/M phase arrest which is p53-independent.

Current cancer treatments including gamma-irradiation, chemotherapy, suicide gene therapy, and immunotherapy, all strongly connect to activation of certain signal pathways that link to apoptosis [34]. Similar to most of agents used in clinics, the induction of apoptosis is the primary mechanism responsible for the anti-HCC effect of DHA. Generally, apoptosis is executed by two pathways, the intrinsic and the extrinsic. The intrinsic pathway, also called mitochondrial pathway, is usually triggered by DNA damage, and the extrinsic pathway, known as the receptor-mediated pathway, is initiated by death receptor activation [18]. DHA has been demonstrated to induce apoptosis through both apoptotic pathways. He et al. [35] reported that DHA, along with



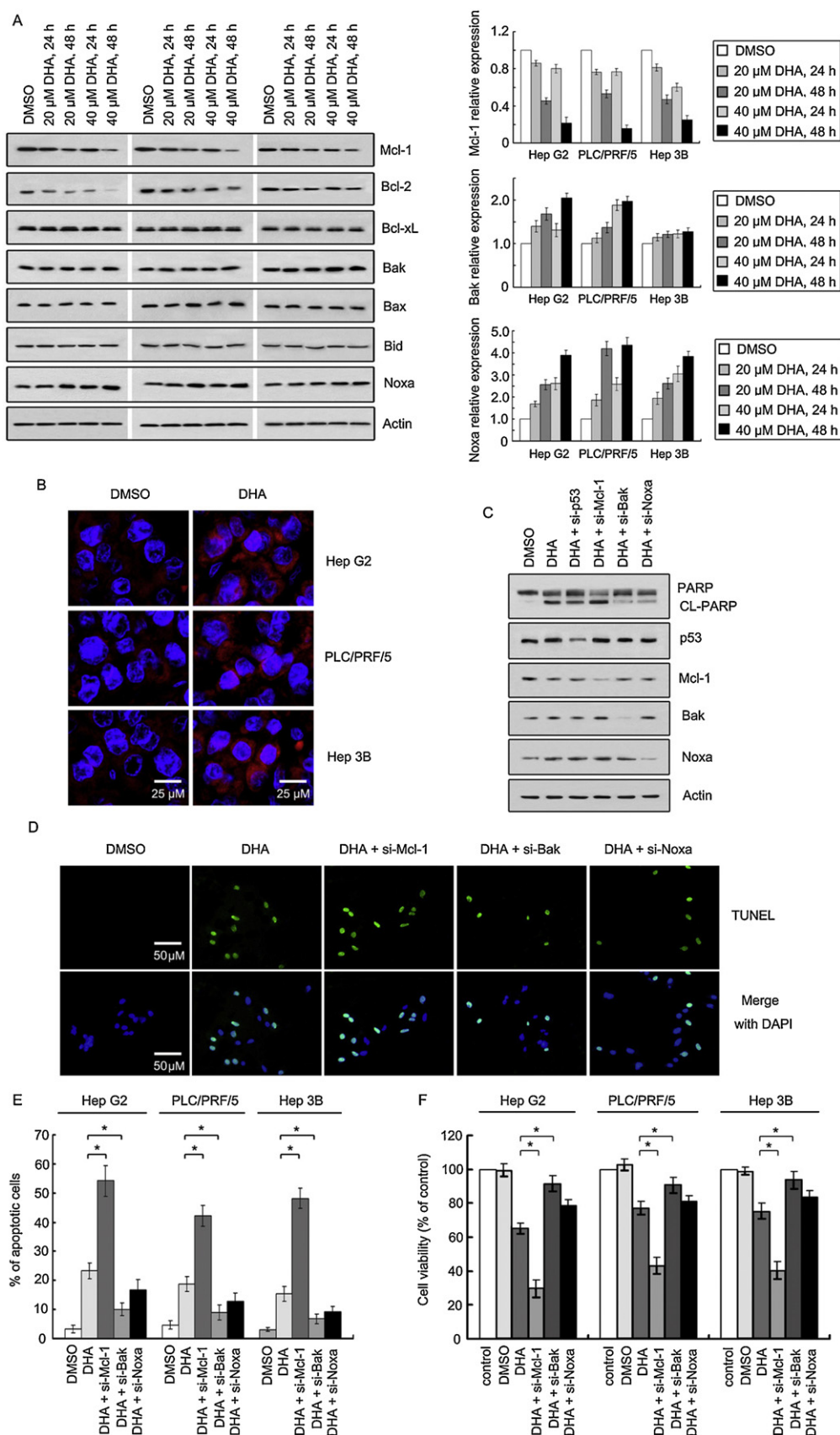


**Fig. 6.** Mcl-1 degradation and Bak activation were associated with DHA-induced apoptosis. (A) Bcl-2 family proteins were involved in DHA-induced apoptosis. HCC cells were treated with DHA for indicated time. The levels of Mcl-1, Bcl-2, Bcl-xL, Bak, Bax, Bid, and Noxa were detected by Western blot. Left panel: A representative result was shown. Right panel: the relative expression of Mcl-1, Bak and Noxa was quantified, according to results of three independent experiments. (B) Bak was activated by DHA treatment. Hep G2 cells were treated with 40  $\mu$ M for 12 h, and then fixed with 4% of PFA. Antibody for active Bak was used to assess the activation of Bak, using immunofluorescence. (C) DHA-induced apoptosis was attenuated by diminishment of Bak or Noxa, but enhanced by decrease of Mcl-1. Hep G2 cells were transfected with siRNA for p53, Mcl-1, Bak or

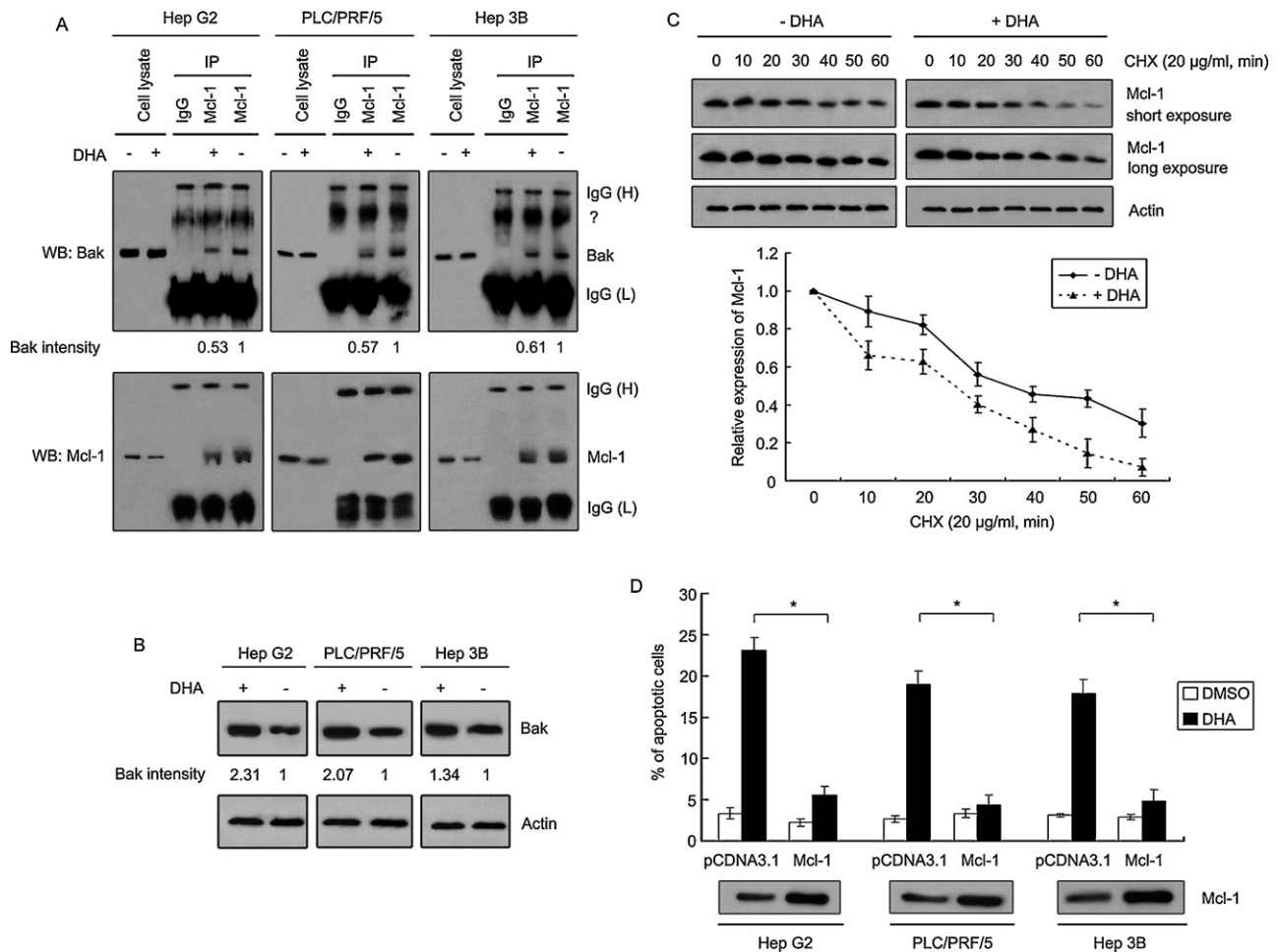


**Fig. 7.** Bak was released from Bak/Mcl-1 complex following DHA treatment. (A) DHA induced a decrease of Bak/Mcl-1 complex. Cells were treated with 40  $\mu$ M DHA for 12 h. Cell lysates were prepared with 1% CHAPS buffer and immunoprecipitated with anti-Mcl-1 antibody or rabbit IgG. Bak and Mcl-1 in precipitated pellets were detected by Western blot. H: Heavy chain; L: Light chain. Levels of endogenous Bak and Mcl-1 in whole-cell lysates (before immunoprecipitation) were also detected. (B) Bak was released from suppressor complexes following DHA treatment. After immunoprecipitated with Mcl-1 antibody, cell lysates were subjected to Western blot to determine the expression of Bak. (C) Degradation of Mcl-1 was enhanced by DHA treatment in Hep G2 cells. Cells were treatment with 40  $\mu$ M DHA for 12 h. Cell lysate was prepared at the indicated time after addition of CHX (20  $\mu$ g/ml) and then subjected to Western blot. (D) Overexpression of Mcl-1 protected HCC cells from DHA-induced cell death. Cells were transfected with pCDNA 3.1 or pCDNA 3.1-Mcl-1 for 18 h, and then treated with 40  $\mu$ M DHA for another 24 h. The means and SD of apoptotic cells from three independent assays were shown. \* $P < 0.05$ .

TRAIL, induced apoptosis in prostate cancer through upregulation of death receptor 5 (DR5). Handrick et al. [15] showed that DHA-induced apoptosis was caspase 9-dependent. In this study, DHA treatment noticeably induced DNA fragmentation and chromatin condensation which are considered as consequences of DNA damage. Furthermore, DHA induced the activation of caspase 9 (an essential initiator of intrinsic apoptosis) but not caspase 8 (an important regulator of extrinsic apoptosis). Sequentially, caspase 3 was activated, leading to the cleavage of poly(ADP-ribose) polymerase (PARP). On the other hand, the release of cytochrome c to cytoplasm from mitochondria, a hallmark of apoptosis, was increased. Furthermore, mitochondrial outer membrane was found to undergo depolarization in response to DHA exposure. Based on the above data, we conclude that DHA induced apoptosis in HCC via the intrinsic pathway.

In view of emerging data that (a) DHA treatment caused mitochondrial membrane depolarization in HCC cells, (b) DHA-

induced apoptosis depended on caspase cascade, and (c) Bcl-2 family proteins are essential regulators of the mitochondrial-relative apoptosis via modulation of mitochondrial membrane permeabilization to control the release of mitochondrial apoptosis inducer, such as cytochrome c and apoptosis-inducing factor (AIF), to the cytoplasm [19,36], we further examined protein levels of some Bcl-2 family members. Our results showed some discrepancies from other reports in altered pattern of Bcl-2 proteins in DHA-exposed cells. For example, Bid, as expected, was not cleaved to from truncated Bid (tBid, active form of Bid that is capable of triggering apoptosis), due to the inactivation of caspase 8. However, Lu et al. [37] reported that DHA induced caspase 8/Bid-dependent apoptosis in ASTC-a-1 cells. DHA is reported to decrease Bcl-xL expression and increase Bax expression in ovarian cancer cell [38], whereas, in our study, the protein levels of antiapoptotic Bcl-xL and proapoptotic Bax remained unchanged. In addition, in HCC cells exposure to DHA resulted in a decline of

Noxa for 18 h, and then cultured with 40  $\mu$ M DHA for another 24 h. Activation of PARP, as well as the expression of p53, Mcl-1, Bak and Noxa, was determined by Western blot. (D) The requirement of Bak and Noxa for DHA-induced apoptosis was further confirmed by TUNEL assay, using *in situ* cell death detection kit. Apoptotic cells were observed under fluorescent microscope. (E) Effects of Mcl-1, Bak and Noxa on apoptosis caused by DHA were examined by TUNEL assay, using flow cytometry. HCC cells transfected with siRNA for 18 h were incubated with 40  $\mu$ M DHA for another 24 h, and then subjected to flow cytometry to assess apoptosis. (F) MTT assay was performed to determine the viabilities of cells treated as described in (E). For (E) and (F). Data are mean  $\pm$  SD of three independent experiments. \* $P < 0.05$ .

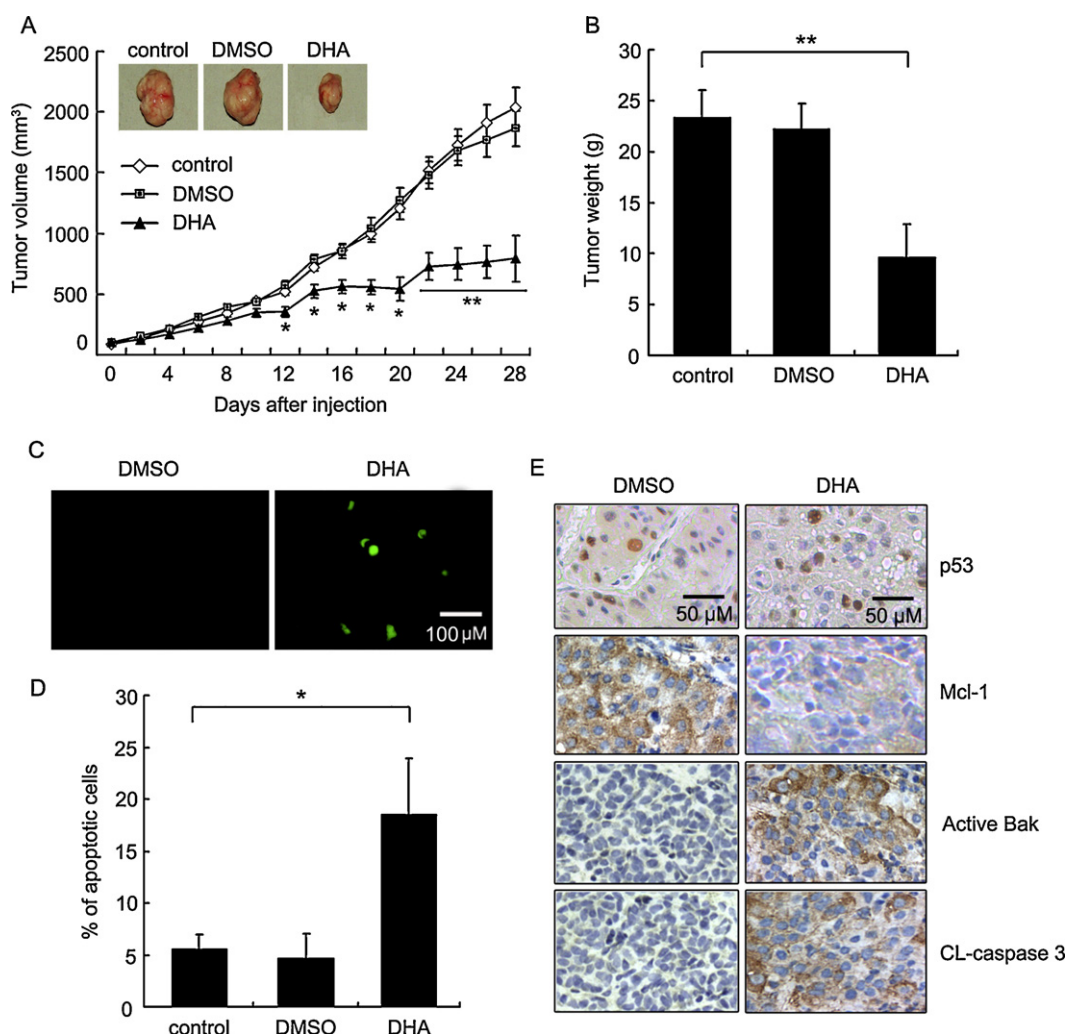


**Fig. 8.** DHA exerted antitumor effect on nude mice bearing Hep G2 xenograft tumor. (A) DHA significantly halted the growth of Hep G2 xenograft tumor. Nude mice were inoculated with  $1 \times 10^7$  of Hep G2 cells. After the formed tumor was palpable, mice were randomly divided into three groups. DHA (20 mg/kg mouse body weight) was given to the DHA group, once daily for five consecutive days per week for 4 weeks. The tumor volumes were calculated every two days. Six xenografts were performed in each group. Data are mean  $\pm$  SD, \* $P < 0.05$ , \*\* $P < 0.01$ , versus the control group. (B) DHA treatment resulted in a dramatic decline of tumor weight. On Day 28, mice were sacrificed, and the tumor weights were measured. (C) DHA induced apoptosis *in vivo*. Tumors were sectioned and apoptosis was determined using *in situ* cell death detection kit. Apoptotic cells were observed under fluorescent microscope. (D) DHA significantly increased apoptosis in DHA-treated mice. Percentages of apoptotic cells were measured by counting the number of green cells under five random fields. \*\* $P < 0.01$ . (E) Decreased expression of Mcl-1 and increased levels of active Bak and cleaved caspase 3 were recorded in DHA-treated mice. Tissues of xenografts were subjected to immunohistochemistry to detect the levels of p53, Mcl-1, active Bak and cleaved caspase 3. Original magnification  $\times 400$ . \* $P < 0.05$ .

antiapoptotic Bcl-2 which was not altered in the study of Handrick et al. [15]. However, our findings are consistent with some other studies. For example, Chen et al. [12] showed that DHA treatment in ovarian cancer cells markedly decreased Bcl-2 expression *in vitro* and *in vivo*. These discrepancies are acceptable and may result from the different pathways via which DHA induces cell growth inhibition in distinct cancer cells that possess their own characteristic systems to regulate apoptosis.

Functionally, Bcl-2 family proteins can be divided two groups: anti-apoptotic proteins (e.g., Bcl-2, Bcl-xL, and Mcl-1) and pro-apoptotic proteins which can be further classified into two subgroups termed multi-domain proteins (e.g., Bax and Bak) and BH3-only proteins (e.g., Bid and Noxa). Bak forms pores in the outer mitochondrial membrane to trigger the release of cytochrome c through a conformational change termed Bak activation. Mcl-1 prevents apoptosis via inhibition of BH3-only proteins by direct interaction to silence their apoptotic activities. However, Mcl-1-mediated resistance to apoptosis can be reversed. Willis et al. [20] showed that Bak was activated through its displacement from Mcl-1 by Noxa. Although the exact mechanism remains unclear, the elucidation of the interaction

among Mcl-1, Bak and Noxa may provide a plausible link to develop new chemotherapeutic drugs for cancer treatment. In parallel with the depolarization of mitochondrial membrane, we found that Bak, which undergoes conformational change and oligomerization to permeabilize the outer membrane of mitochondria, was activated in response to DHA. Coincidentally, a rapid decline of Mcl-1, which is clearly demonstrated as an effective inhibitor of Bak, was observed.

Though DHA could induce apoptosis in all three HCC cell lines, more apoptosis was observed in wild-type p53-expressing cells (Hep G2), compared to other two types of cells (mutant p53 protein in PLC/PRF/5 cells and no p53 protein in Hep 3B cells). Furthermore, wild-type p53 was upregulated while mutant p53 was down-regulated in DHA-exposed cells. These data suggest that p53 may partly but not essentially contribute to DHA-induced apoptosis. p53 has been shown to facilitate some agents to inhibit cancer cells. Spinnler et al. [39] reported that p53 potentiated apoptosis via abrogation of Wip 1 in human tumor cells. Gurzov et al. [40] demonstrated that p53 contributed to apoptosis induced in pancreatic beta-cell by upregulating PUMA. Here we reported that p53 facilitated DHA-induced apoptosis because DHA-induced



apoptosis was greatly enhanced in Hep 3B cells with ectopic expression of p53, but significantly attenuated in Hep G2 cells with RNAi-mediated diminishment of p53. It is possible that the sensitivity to DHA treatment by p53 is associated with p53-induced regulation of Bak. Mitochondrial p53 can interact with and subsequently activate Bak, resulting in release of cytochrome c from mitochondria [41]. On the other hand, p53 may potentiate Bak oligomerization to induce cell death [42,43]. Lately, p53 is reported to induce endogenous Bak at both mRNA and protein levels [44]. However, how p53 facilitates DHA-induced apoptosis and whether p53 mediates Bak activation in DHA-exposed cells require further investigations. These data may suggest a potential strategy for HCC chemotherapy.

Consistent with the significant inhibition of tumor growth *in vitro*, the administration of DHA to HCC xenograft tumor in nude mice pronouncedly halted the tumor growth. Our finding is in line with other reports. Wang et al. [13] showed that DHA significantly reduced the tumor volume. Gao et al. [16] reported that DHA dramatically inhibited U937 xenograft tumor. In conclusion, our *in vitro* and *in vivo* data indicate that DHA possesses unique proapoptotic features and appears to be a promising anti-HCC agent.

## References

- [1] Parkin DM, Bray F, Ferlay J, Pisani P. Global cancer statistics, 2002. *CA Cancer J Clin* 2005;55:74–108.
- [2] Bosch FX, Ribes J, Diaz M, Cleries R. Primary liver cancer: worldwide incidence and trends. *Gastroenterology* 2004;127:S5–16.
- [3] Erichsen R, Jepsen P, Jacobsen J, Norgaard M, Vilstrup H, Sorensen HT. Time trends in incidence and prognosis of primary liver cancer and liver metastases of unknown origin in a Danish region, 1985–2004. *Eur J Gastroenterol Hepatol* 2008;20:104–10.
- [4] Villanueva A, Llovet JM. Targeted therapies for hepatocellular carcinoma. *Gastroenterology* 2011;140:1410–26.
- [5] Hutchinson L. Targeted therapies: doxorubicin and sorafenib improves survival in patients with advanced hepatocellular carcinoma. *Nat Rev Clin Oncol* 2011;8:61.
- [6] Rahbari NN, Mehrabi A, Mollberg NM, Muller SA, Koch M, Buchler MW, et al. Hepatocellular carcinoma: current management and perspectives for the future. *Ann Surg* 2011;253:453–69.
- [7] Breous E, Thimme R. Potential of immunotherapy for hepatocellular carcinoma. *J Hepatol* 2011;54:830–4.
- [8] Giannelli G, Mazzocca A, Fransvea E, Lahn M, Antonaci S. Inhibiting TGF-beta signaling in hepatocellular carcinoma. *Biochim Biophys Acta* 2011;1815:214–23.
- [9] Eastman RT, Fidock DA. Artemisinin-based combination therapies: a vital tool in efforts to eliminate malaria. *Nat Rev Microbiol* 2009;7:864–74.
- [10] Dondorp AM, Fairhurst RM, Slutsker L, Macarthur JRMDJ, Guerin JP, et al. The threat of artemisinin-resistant malaria. *N Engl J Med* 2011;365:1073–5.
- [11] Mu D, Zhang W, Chu D, Liu T, Xie Y, Fu E, et al. The role of calcium, P38 MAPK in dihydroartemisinin-induced apoptosis of lung cancer PC-14 cells. *Cancer Chemother Pharmacol* 2008;61:639–45.
- [12] Chen T, Li M, Zhang R, Wang H. Dihydroartemisinin induces apoptosis and sensitizes human ovarian cancer cells to carboplatin therapy. *J Cell Mol Med* 2009;13:1358–70.
- [13] Wang SJ, Gao Y, Chen H, Kong R, Jiang HC, Pan SH, et al. Dihydroartemisinin inactivates NF-kappaB and potentiates the anti-tumor effect of gemcitabine on pancreatic cancer both *in vitro* and *in vivo*. *Cancer Lett* 2010;293:99–108.
- [14] Ji Y, Zhang YC, Pei LB, Shi LL, Yan JL, Ma XH. Anti-tumor effects of dihydroartemisinin on human osteosarcoma. *Mol Cell Biochem* 2011;351:99–108.
- [15] Handrick R, Ontikatz T, Bauer KD, Freier F, Rubel A, Durig J, et al. Dihydroartemisinin induces apoptosis by a Bak-dependent intrinsic pathway. *Mol Cancer Ther* 2010;9:2497–510.
- [16] Gao N, Budhraj A, Cheng S, Liu EH, Huang C, Chen J, et al. Interruption of the MEK/ERK signaling cascade promotes dihydroartemisinin-induced apoptosis *in vitro* and *in vivo*. *Apoptosis* 2011;16:511–23.
- [17] Zhang CZ, Zhang HT, Chen GG, Lai PB. Trichostatin A sensitizes HBx-expressing liver cancer cells to etoposide treatment. *Apoptosis* 2011;16:683–95.
- [18] Landgraaber S, von Knoch M, Loer F, Wegner A, Tsokos M, Hussmann B, et al. Extrinsic and intrinsic pathways of apoptosis in aseptic loosening after total hip replacement. *Biomaterials* 2008;29:3444–50.
- [19] Chai WS, Zhu XM, Li SH, Fan JX, Chen BY. Role of Bcl-2 family members in caspase-3/9-dependent apoptosis during *Pseudomonas aeruginosa* infection in U937 cells. *Apoptosis* 2008;13:833–43.
- [20] Willis SN, Chen L, Dewson G, Wei A, Naik E, Fletcher JL, et al. Proapoptotic Bak is sequestered by Mcl-1 and Bcl-xL, but not Bcl-2, until displaced by BH3-only proteins. *Genes Dev* 2005;19:1294–305.
- [21] Gelinas C, White E. BH3-only proteins in control: specificity regulates MCL-1 and BAK-mediated apoptosis. *Genes Dev* 2005;19:1263–8.
- [22] van Delft MF, Wei AH, Mason KD, Vandenberg CJ, Chen L, Czabotar PE, et al. The BH3 mimetic ABT-737 targets selective Bcl-2 proteins and efficiently induces apoptosis via Bak/Bax if Mcl-1 is neutralized. *Cancer Cell* 2006;10:389–99.
- [23] Du X, Youle RJ, FitzGerald DJ, Pastan I. *Pseudomonas* exotoxin A-mediated apoptosis is Bak dependent and preceded by the degradation of Mcl-1. *Mol Cell Biol* 2010;30:3444–52.
- [24] Lai H, Sasaki T, Singh NP, Messay A. Effects of artemisinin-tagged holotransferrin on cancer cells. *Life Sci* 2005;76:1267–79.
- [25] Willoughby Sr JA, Sundar SN, Cheung M, Tin AS, Modiano J, Firestone GL. Artemisinin blocks prostate cancer growth and cell cycle progression by disrupting Sp1 interactions with the cyclin-dependent kinase-4 (CDK4) promoter and inhibiting CDK4 gene expression. *J Biol Chem* 2009;284:2203–13.
- [26] Wuari J, Buck V, Nurse P, Millar JB. Stable association of mitotic cyclin B/Cdc2 to replication origins prevents endoreduplication. *Cell* 2002;111:419–31.
- [27] Zwicker J, Lucibello FC, Wolfrum LA, Gross C, Truss M, Engeland K, et al. Cell cycle regulation of the cyclin A, cdc25C and cdc2 genes is based on a common mechanism of transcriptional repression. *EMBO J* 1995;14:4514–22.
- [28] Goss VL, Cross JV, Ma K, Qian Y, Mola PW, Templeton DJ. SAPK/JNK regulates cdc2/cyclin B kinase through phosphorylation and inhibition of cdc25c. *Cell Signal* 2003;15:709–18.
- [29] Song X, Kim HC, Kim SY, Basse P, Park BH, Lee BC, et al. Hyperthermia-enhanced TRAIL- and mapatumumab-induced apoptotic death is mediated through mitochondria in human colon cancer cells. *J Cell Biochem* 2012. in press.
- [30] Kim S, Lee HS, Lee SK, Kim SH, Hur SM, Kim JS, et al. 12-O-Tetradecanoyl phorbol-13-acetate (TPA)-induced growth arrest is increased by silibinin by the down-regulation of cyclin B1 and cdc2 and the up-regulation of p21 expression in MDA-MB231 human breast cancer cells. *Phytomedicine* 2010;17:1127–32.
- [31] Jo HJ, Song JD, Kim KM, Cho YH, Kim KH, Park YC. Diallyl disulfide induces reversible G2/M phase arrest on a p53-independent mechanism in human colon cancer HCT-116 cells. *Oncol Rep* 2008;19:275–80.
- [32] Manna SK, Bose JS, Gangan V, Raviprakash N, Navaneetha T, Raghavendra PB, et al. Novel derivative of benzofuran induces cell death mostly by G2/M cell cycle arrest through p53-dependent pathway but partially by inhibition of NF-kappaB. *J Biol Chem* 2010;285:22318–27.
- [33] Meng L, Hsu JK, Tsai RY. GNL3L depletion destabilizes MDM2 and induces p53-dependent G2/M arrest. *Oncogene* 2011;30:1716–26.
- [34] Fulda S, Debatin KM. Extrinsic versus intrinsic apoptosis pathways in anticancer chemotherapy. *Oncogene* 2006;25:4798–811.
- [35] He Q, Shi J, Shen XL, An J, Sun H, Wang L, et al. Dihydroartemisinin upregulates death receptor 5 expression and cooperates with TRAIL to induce apoptosis in human prostate cancer cells. *Cancer Biol Ther* 2010;9:819–24.
- [36] Brunelle JK, Letai A. Control of mitochondrial apoptosis by the Bcl-2 family. *J Cell Sci* 2009;122:437–41.
- [37] Lu YY, Chen TS, Qu JL, Pan WL, Sun L, Wei XB. Dihydroartemisinin (DHA) induces caspase-3-dependent apoptosis in human lung adenocarcinoma ASTC-a-1 cells. *J Biomed Sci* 2009;16:16.
- [38] Jiao Y, Ge CM, Meng QH, Cao JP, Tong J, Fan SJ. Dihydroartemisinin is an inhibitor of ovarian cancer cell growth. *Acta Pharmacol Sin* 2007;28:1045–56.
- [39] Spinnler C, Hedstrom E, Li H, de Lange J, Nikulenkov F, Teunisse AF, et al. Abrogation of Wp1 expression by RITA-activated p53 potentiates apoptosis induction via activation of ATM and inhibition of HdmX. *Cell Death Differ* 2011;18:1736–45.
- [40] Gurzov EN, Germano CM, Cunha DA, Ortis F, Vanderwinden JM, Marchetti P, et al. p53 up-regulated modulator of apoptosis (PUMA) activation contributes to pancreatic beta-cell apoptosis induced by proinflammatory cytokines and endoplasmic reticulum stress. *J Biol Chem* 2010;285:19910–20.
- [41] Leu JI, Dumont P, Hafey M, Murphy ME, George DL. Mitochondrial p53 activates Bak and causes disruption of a Bak-Mcl1 complex. *Nat Cell Biol* 2004;6:443–50.
- [42] Pietsch EC, Leu JI, Frank A, Dumont P, George DL, Murphy ME. The tetramerization domain of p53 is required for efficient BAK oligomerization. *Cancer Biol Ther* 2007;6:1576–83.
- [43] Pietsch EC, Perchiniak E, Canutescu AA, Wang G, Dunbrack RL, Murphy ME. Oligomerization of BAK by p53 utilizes conserved residues of the p53 DNA binding domain. *J Biol Chem* 2008;283:21294–304.
- [44] Graupner V, Alexander E, Overkamp T, Rothfuss O, De Laurenzi V, Gillissen BF, et al. Differential regulation of the proapoptotic multidomain protein Bak by p53 and p73 at the promoter level. *Cell Death Differ* 2011;18:1130–9.